Biomaterials 33 (2012) 7686–7698

Contents lists available at SciVerse ScienceDirect

Biomaterials

journal homepage: www.elsevier.com/locate/biomaterials

Functional replication of the tendon tissue microenvironment by a bioimprinted substrate and the support of tenocytic differentiation of mesenchymal stem cells

Wing Yin Tong [a,1], Wei Shen [b,1], Connie W.F. Yeung [b], Ying Zhao [c], Shuk Han Cheng [b], Paul K. Chu [c], Danny Chan [d], Godfrey C.F. Chan [e], Kenneth M.C. Cheung [a], Kelvin W.K. Yeung [a,*], Yun Wah Lam [b,*]

[a] Departments of Orthopaedics & Traumatology, The University of Hong Kong, Hong Kong, China
[b] Departments of Biology & Chemistry, City University of Hong Kong, Hong Kong, China
[c] Physics & Materials Science, City University of Hong Kong, Hong Kong, China
[d] Departments of Biochemistry, The University of Hong Kong, Hong Kong, China
[e] Paediatrics & Adolescent Medicine, The University of Hong Kong, Hong Kong, China

ARTICLE INFO

Article history:
Received 20 May 2012
Accepted 1 July 2012
Available online 19 July 2012

Keywords:
Bioimprinting
Mesenchymal stem cells
Tendon
Tissue microenvironment
ECM
Biomimetic material

ABSTRACT

Although many studies have demonstrated that cell phenotype is affected by the surface properties of biomaterials, these materials often fail to mimic the complexity of the native tissue microenvironment (TME). In this study, we have developed a new experimental model that allows the characterisation and functional reconstruction of natural TME. We discovered that mesenchymal stem cells (MSC) cultured on cryostat sections of bovine Achilles tendon adopted an elongated and aligned morphology, and expressed tenocyte marker tenomodulin (TNMD). This suggests that tendon sections contain the signalling cues that guide MSCs to commit to the tenogenic lineage. To reconstruct this instructive niche, we prepared PDMS replica by using tendon sections as template. The resulting bioimprint faithfully copied the physical topography and elasticity of the section. This replica, when coated with collagen 1, supported tenogenesis of MSC without requiring exogenous growth factors. This study illustrates how extracellular biophysical and biochemical features intertwines to form a niche that influences the cell fate and demonstrated that such complex information could be conveniently reconstructed with synthetic materials and purified extracellular matrix proteins.

1. Introduction

Tissue engineering is an emerging field in which materials science and stem cell biology corroborate to fulfil the promise of regenerative medicine. Its ultimate goal is to recapitulate the natural process of tissue formation by assembling cells onto synthetic scaffolds [1], which mimic the native tissue microenvironment (TME). The crux of this multidisciplinary challenge is the need to understand how cell behaviours are regulated through cell-TME interactions [2,3], and to translate such understandings to the fabrication of biomaterials [4].

The biochemical building block of the TME is the extracellular matrix (ECM), a complex mixture of proteins and glycosaminoglycans. Some of these factors regulate cell functions by directly interacting with specific surface receptors, while others are required for the assembly of extracellular scaffolds that transmit the appropriate mechano-transduction signals to the cells. Numerous studies have demonstrated the level of control commanded by ECM over cellular behaviours. For example, mouse embryonic stem cells (ESC) seeded on ECM isolated from osteogenic cell line MC3T3E1 differentiated into osteoblasts more efficiently than on ECM from a non-osteogenic cell line [5]. This suggests that ECMs contain biological cues that can instruct cell lineage commitment. Furthermore, the spatial dimensions, topographical geometry and mechanical features of the cell culture substratum can also profoundly affect cellular behaviours, such as adhesion [6], migration [7], and differentiation [8]. For example, matrix elasticity can influence differentiation of both mesenchymal stem cells (MSC) [9] and haematopoietic stem cells [10]. Substrate roughness can also influence the differentiation of osteoblasts, both in vitro [11], and in vivo [12]. More recently, surface wettability, topography, chemistry and indentation elastic modulus have all been shown to affect ESC differentiation [13].

* Corresponding authors.
E-mail addresses: wkkyeung@hku.hk (K.W.K. Yeung), yunwlam@cityu.edu.hk (Y.W. Lam).
[1] These authors equally contributed to this work.

0142-9612/$ – see front matter © 2012 Elsevier Ltd. All rights reserved.
http://dx.doi.org/10.1016/j.biomaterials.2012.07.002

These studies have established the general principle that both biochemical signals in TME, in terms of ECM compositions, and its physical architecture, in terms of substrate chemistry and topography, play determining roles in regulating cell phenotypes. However, most existing experimental models on TME are reductionistic and oversimplifying [4]. For example, even the largest ECM microarray screening experiment to date [14] had studied the effect of the combination of only 5 ECM proteins on stem cell differentiation. This kind of study can never reflect the biochemical complexity of the natural TME, as a recent proteomic characterisation of ECM scaffold isolated from human breast tissues has led to the identification of over 4000 proteins [15]. Furthermore, observations of cell-ECM interactions are typically made from cells seeded on a culture dish coated with a layer of ECM components, or at best, enveloped in a homogenous ECM gel. Convenient as it is, this approach presents cells with ECM proteins in unnatural topographical configurations [16], and often fails to recapitulate physiological cellular behaviours and functions [17]. Micropatterning and electrospinning produce simple and regular surfaces that rarely resemble any real biological structures and cannot mimic the complex and intricate architecture of the endogenous TME. It is therefore difficult to judge how the knowledge obtained from these models can be translated into tissue engineering applications.

The major gap in knowledge in the field of tissue engineering is the lack of an experimental model for the study of cell-TME interactions that allows for the effective characterisation of cellular phenotypes while faithfully reflecting the complexity of native TME. Without such a model system, many fundamental questions on the roles of TME will remain unanswered, and rational strategies for the TME reconstruction cannot be developed. For instances, what are the contributions of biochemical and mechanical signals in a TME in tissue formation? How should artificial materials be constructed to mimic the correct combination of these signals? To address these questions, we aimed to develop a model system that can define, as well as reconstruct, how the native ECM regulates cell phenotypes. Using bovine Achilles tendon as a proof-of-concept model, we tested the feasibility of using histological sections of organs to provide the TME for cell culture. We further explored the use of bioimprinting and extracellular matrix protein coating to functionally replicate this TME. We believe the knowledge presented here would be beneficial to the further biomaterial design and application.

2. Materials and methods

2.1. Preparation of native microenvironment from tissue sections

Fresh bovine Achilles tendon was obtained from a local food market. The tendon was trimmed into tissue blocks of about 1 cm × 1 cm × 1 cm in size and stored at −80 °C. Before the cell culture experiments, the blocks were mounted onto the tissue holder of a cryostat (JUNG CM 1500, Leica Instruments) with polyvinyl alcohol and polyethylene glycol (OCT, Jung, 0201 08926). The mounting orientation was carefully adjusted so that the tendon blocks were either longitudinally or transversely cut (see below). Cryosections that were 25 μm in thickness were thawed onto glass slides (Menzel-Glaser Superfrost Ultra Plus). Longitudinal and cross sections of tendon blockes were positioned on the same slide. In order to standardise the cell seeding areas, a hydrophobic blocker (Mini PAP Pen, Invitrogen) was used to mark 2 × 2.5 cm^2 rectangles around each section. The sections were washed thoroughly with phosphate buffered saline (PBS) and mildly fixed with 4% paraformaldehyde (PFA, Sigma–Aldrich) in PBS for 15 min at room temperature. It was followed glycine quenching (100 mM Glycine in PBS, USB) twice (15 min each) to neutralize free aldehyde groups. The slides were further washed three more times with PBS for 5 min each.

2.2. Cell culture

TERT-immortalised human MSC stably expressing GFP [18] were a kind gift from Dr Dario Campana (St. Jude Children's Research Hospital, Memphis, USA). MC3T3E1, NIH3T3, MCF7, MDCK and HeLa cells were obtained from American Type Culture Collection (ATCC number CRL-2594, CRL-1658, HTB-22, CCL-34 and CCL-2 respectively). Except for the MSCs, the cells were maintained in Dulbecco's modified eagle medium (DMEM) – high glucose (Invitrogen, 11995-065) with 10% fetal calf serum. The MSC were maintained in DMEM – low glucose (Invitrogen, 31600-026) supplemented with 10% heat inactivated fetal calf serum (Invitrogen), 1% Antibiotic-Antimycotic (Invitrogen) at 37 °C and 5% CO_2 in a humidified incubator. Confluence was kept under 80% at all times, and the media were refreshed every three days. Only MSCs at passages 6–10 were used for the experiments. The cells were seeded at 10^4 cells/cm^2 on the tendon sections and bioimprints, and were maintained in their respective normal DMEM supplemented with 75 μg/ml of ascorbic acids.

2.3. Atomic force microscopy (AFM)

The tendon sections were prepared as described for the cell culture experiments, and immersed into PBS at room temperature. The surface architecture and mechanical properties of the sections were imaged by using a BioScope Catalyst atomic force microscope (Bruker AXS) equipped with a Tap 150A probe (Veeco Instruments, Inc., Plainview, NY) in tapping mode according to the manufacturer's instructions. Mechanical properties mappings were taken under PeakForce QNM imaging mode. Images were analysed by NanoScope Analysis (Bruker) software.

2.4. Scanning electron microscopy (SEM)

The tendon sections were prepared as described for the cell culture experiments, and were immersed into PBS at room temperature. Fixed samples were dehydrated through a series of increasing ethanol concentrations, followed by 3 changes of hexamethyldisilasane (HMDS, Sigma Aldrich, H4875), and then dried against filter paper. The samples were carbon coated by evaporation. The coated samples were imaged under an environmental scanning electron microscope (FEI/Philips XL30 Esem-FEG).

2.5. Cell adhesion assay

The cultured cells were seeded at a density of 10^4 cells/cm^2 for 1 h (2 h for htMSCs) followed by rinsing with pre-warmed PBS. The remaining cells were imaged under a fluorescence microscope (Leica DMI 3000 B). At least three images were randomly taken on each sample. The cell number was counted with NIH ImageJ (see below). To aid visualisation of cells in some of the experiments, seeded cells were initially labelled with mitotracker (Invitrogen, M7512) for 15 min. The pilot study showed that there is no significant difference on cell adhesion between pre-labelled cells and normal cells (data not shown).

2.6. S-phase labelling

To compare the proliferating rate of the cells on the sections, the proportion of S-phase cells for a period of time was measured. Click EdU Alexa 488 imaging kit (Invitrogen, C10337) was used for labelling of S-phase cells on sections. The procedure followed the description in the manual. To exclude cells that remained inside the tissue, the sections were counter labelled with dead stain from a live/dead staining kit. The images were taken under a microscope (Leica confocal microscope SP5), and counted through image analysis. The reported proportion of the S-phase was defined as the number of S-phase labelled cells/total number of cells.

2.7. Immunofluorescence

The cells were seeded on to the sections as described. After a duration of time, cells were fixed for 5 min with 4% freshly prepared PFA at room temperature, quenched with 100 mM glycine in PBS for 15 min and washed twice with PBS before permeablisation in 1% Triton X-100 in PBS for 2 min at room temperature. After permeablisation, the cells were washed twice in PBS and blocked with 1% bovine serum albumin (BSA) in PBS for 30 min at room temperature. The cells were then incubated with primary antibodies for 60 min, washed, and incubated with fluorochrome-conjugated secondary antibodies for 60 min. The slides were washed in PBS followed by counter staining for 15 min. The primary antibodies used were mouse anti-vinculin, mouse anti-integrin β1, anti-integrin α3 (Millipore, MAB3574, MAB1965 and MAB1952P respectively) and rabbit anti-tenomodulin (Santa-Cruz, SC-98875). The secondary antibodies used were Alexa 488 goat anti-rabbit, Alexa 546 donkey anti-mouse and Alexa 647 donkey anti rabbit (Invitrogen, A211008, A10036 and A31573, respectively). Rhodamine-phalloidin (Invitrogen, R415) and Hoechst (Sigma Aldrich, B2261) were used to counter label the filament actin and nucleus, respectively. For images that showed only the cell morphology, the cells surface was labelled by a live/dead cytotoxicity assay kit (Invitrogen L7012).

2.8. Western blotting

The cells that were attached to the sections were trypsinized for 5 min, The cells in suspension were collected, washed in warm PBS, and lysed in a sodium dodecyl sulphate (SDS) buffer (2% SDS, 50 nM Tris pH 6.8). The trypsinised cell suspension

was gently passed through a 70 μm filter to remove any protein fragments from the sections. The protein concentration was quantified by an EZQ protein quantitation kit (Invitrogen, R3320). The proteins were mixed with an SDS loading buffer, followed by separation with 10% Novex precast gel (Invitrogen) at 100 V, and transferred onto a nitrocellulose membrane. The membrane was blocked with 5% (w/v) nonfat milk powder (Nestle) and 0.05% Tween-20 in PBS for 60 min, followed by washing with 0.05% Tween-20 in PBS and incubated with a primary antibody in a blocking buffer for 2 h. The primary antibodies used were mouse anti-collagen 1, rabbit anti-SOX9, rabbit anti-ALP, rabbit anti-tenomodulin (Abcam, ab34710, ab26414, ab95462 and ab81328 respectively), rabbit anti-fibronectin and mouse anti-tubulin (Santa-Cruz, SC-9068 and SC-32293 respectively). The secondary antibodies used were horseradish peroxidase conjugated anti-mouse immunoglobulin G (GE Healthcare) and anti-rabbit immunoglobulin G (GE Healthcare). The membrane was washed and incubated with the secondary antibodies for 60 min. After washing, the membrane was developed with an Amersham Biosciences ECL Plus™ detection kit (GE Healthcare) and imaged by using a Gel Doc with a cool CCD camera (Fujifilm LAS-3000, Fujifilm Corporation, Tokyo, Japan).

2.9. Time-lapse microscopy

The MSCs were seeded at 10^4 cells/cm^2 on the tendon sections and imaged with a laser scanning confocal microscope (Leica TCS SP5) for every 6 min from 1 to 14 h post-seeding. During imaging, the cells were maintained in a CO_2 independent medium (Invitrogen) in a humidified 37 °C environment.

2.10. Tissue bioimprinting and plasma treatment

Bioimprints were fabricated to reproduce the topology of a TME on polydimethylsiloxane (PDMS). The fabrication procedure was optimised based on a protocol described by Muys et al. [19]. PDMS (Dow Corning Sylgard 184, 4019862) was mixed at a ratio of 100:3 or 100:30 base to curing agent to represent different stiffnesses. They were degased for 20 min at room temperature. The tissue sections were prepared as described and the PBS was aspirated, followed by application of the degased PDMS mix. They were pre-cured for 2 min at 95 °C, followed by incubation at 37 °C for 2 h. The resulting negative imprint was peeled off from the tissue and cleaned by sonication in water for 30 min. Silanisation of the imprint was carried out by putting it under a vacuum together with 100 μl of trichloro (1,1,2,2-perfluoocytl) for 2 h. The negative imprint was then served as the template, and the positive replica was casted by repeating the casting procedure. The positive replica was treated an O_2 plasma immersion in a multiple purpose ion implantation/coating and immersion system as specified by Wang et al. [20]. Treatment was conducted under 100 sccm supply of O_2 at 200 W RF ionisation power. The working pressure was 6.2×10^{-1}Pa. The duration of immersion was 5 min. The treatment was verified by water contact angle measurement, which measured around 70° after treatment. The topography was measured by AFM as described above. The positive replica was cleaned by sonication and stored under MilliQ before use [21].

2.11. BSA blocking experiments

The blocking of tissue sections was performed to study the role of biochemical cues. The tendon sections were prepared as described above. The sections were incubated with 10% BSA in PBS at 4 °C overnight. The sections were then washed three times with PBS and mildly fixed with 4% PFA in PBS for 15 min, followed by quenching with 100 mM glycine in PBS. The blocked sections were further washed in PBS for three times for 5 min each time before the cell culture experiments.

2.12. Collagen coating of cryosection replicas

Replicas were coated with rat tail collagen 1 (invitrogen A10483) according to the product manual. Briefly, sterilized replicas were placed in 12 well plates, and collagen 1 concentration was carefully adjusted by 0.02M acetic acid such that the coating concentration was either 88 μg/cm2 or 8.8 μg/cm2 for 1 h at room temperature. After incubation, the bioimprints were washed with equal volume of PBS for 3 times to adjust the acidity. The coated imprints were dried briefly and used as culture substrate immediately.

2.13. Image analysis

Image analysis was performed to quantify cell number, staining intensity and alignment, elongation, and spreading area from images. The images obtained were analysed by NIH ImageJ (version 1.42q) and Macnification (version 1.7.1). To measure the cell staining intensity, the cells were first recorded as a region of interest (ROI). The staining intensity of each ROI was then measured. For cell counting, ROI was defined as nucleus staining and the number of ROIs was reported. For cell elongation, the average aspect ratio of cells (long axis/short axis) was measured. For cell alignment quantification, a reference line was arbitrarily defined. The angle between the reference line and major axis of cells was measured. The relative alignment, defined as the reciprocal of a standard error of the average angle, was reported. The averages of measurements were taken from at least 100 cells that were randomly selected from each sample.

2.14. Statistical analysis

All quantitative data presented in this report are based on triplicated experiments. In all cases, the means among the groups were compared by student *t*-test. The hypothesis was accepted at a 95% significant level ($p > .05$).

3. Results

3.1. Tissue sections contain exposed tissue microenvironment

In this study, we have sought to develop a system to, firstly, define the roles of TME in cellular functions and behaviours, and to reconstruct those TME by using synthetic materials. This work was initiated by our observation that MSC adopted highly distinct morphology when seeded directly on cryostat sections of trabecular bone, cartilage and tendon (Fig. 1A). We interpreted this phenomenon as an indication that these histological sections displayed the unique biochemical and physical features characteristic of individual TME. We focused our investigations on Achilles tendon, as it is a more structurally organised tissue, and therefore ideal for proof of concept. Cryosections of bovine Achilles tendon exhibit a highly intact histology, in the form of closely packed collagen fibrils with sparsely distributed tenocytes aligned along the extracellular fibrils (Fig. 1B). SEM (Fig. 1C) and AFM (Fig. 1D) reveal detailed fibrillar topographies on these sections. Many previous studies have used decellularised tissues as cell culture scaffolds [22,23]. However, SEM shows that the decellularisation procedure causes a dramatic disruption in the tendon ultrastructure (Suppl Fig. 1), a problem that consistently occurs in other decellularised tissues [24]. Compared to decellularised tendon, histological sections exhibited a much better preserved tissue architecture and are more likely to represent the TME.

3.2. Cell type-dependent responses to tendon cryosections

To investigate how the tendon TME affects cellular behaviours, we cultured various mammalian cell lines, namely, mouse fibroblasts (MC3T3E1 and NIH3T3), human carcinoma cells (MCF7 and HeLa), canine epithelial cells (MDCK), and human MSC, onto tendon sections and glass surface. All cell lines efficiently adhered and spread onto the sections. As all endogenous cells in the sections were dead (data not shown), they would not interfere with the cell culture experiments.

MC3T3E1, NIH3T3 and MSC were significantly more elongated on the tendon sections (Fig. 1E). The aspect ratio measurements indicated that these cells were more elongated on the tendon sections than on the glass control by over two folds (Fig. 1F), despite no detectable difference in cell size on these two surfaces (Suppl Fig. 2). In contrast, the MCF7, MDCK and HeLa cells were not elongated on the tendon sections (Fig. 1F). Hence, it implies that the surface of tendon sections contain features that selectively induce elongation and alignment of fibroblast-like cells (e.g. MC3T3E1, NIH3T3 and MSC), whereas no such effect was observed for epithelial-like cells (e.g. HeLa, MCF7 and MDCK).

Supplementary data related to this article can be found online at http://dx.doi.org/10.1016/j.biomaterials.2012.07.002.

We examined the MSC and MC3T3E1 cells on tendon sections by SEM. MSC appear to spread over the section surface (Fig. 2A), with cell protrusions adhering on individual sites on the collagen fibrils (Fig. 2A, arrows). The dynamics of cell adhesion of MSC on the tendon sections were further examined by time-lapse microscopy. We took advantage of the expression of GFP in these cells to visualise cell movement and spreading on the sections. During the first

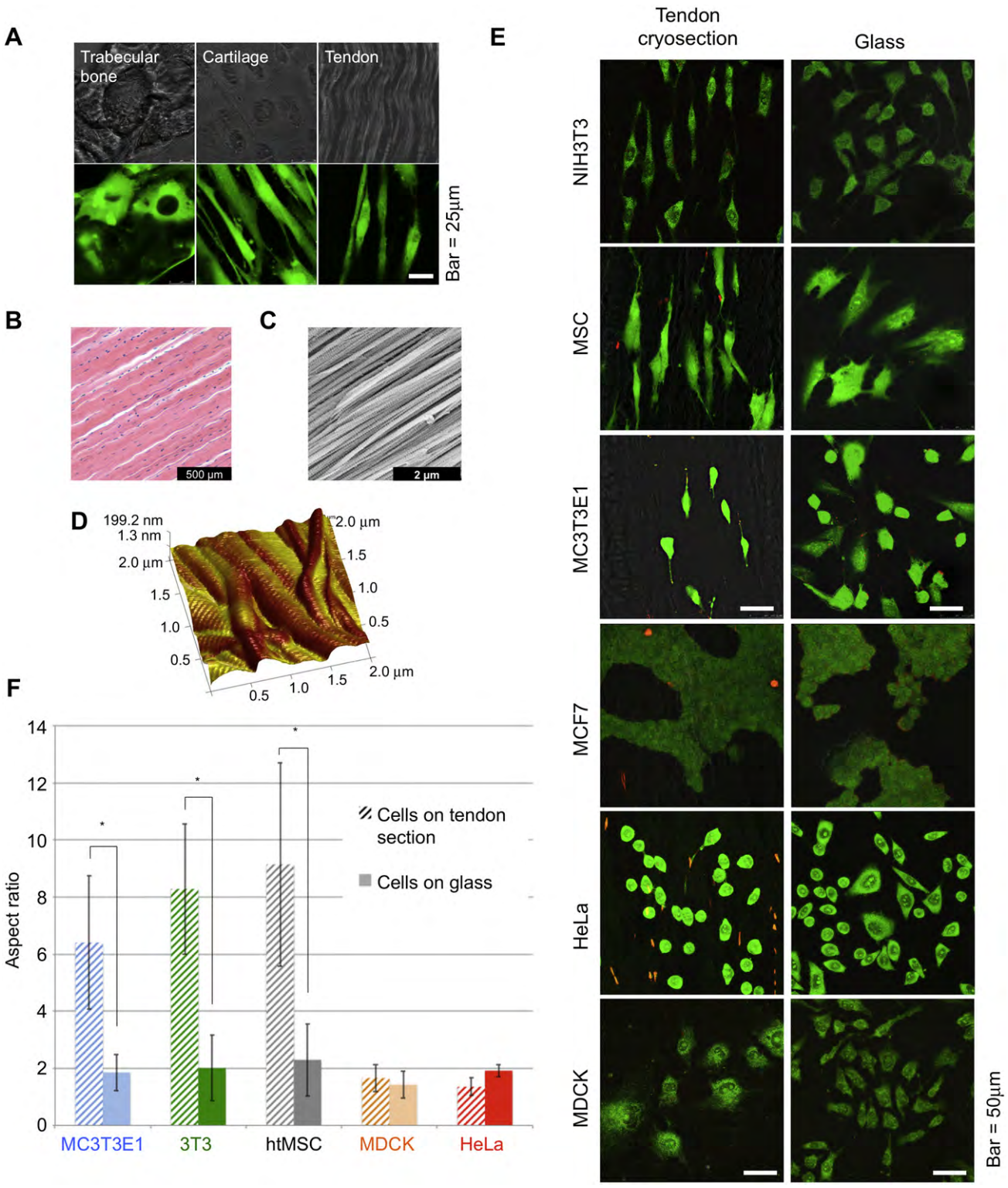

Fig. 1. (A) Morphology of MSCs on trabecular bone, cartilage and Achilles tendon tissue cryosections. Upper row: DIC images. Lower row: GFP images. (B) H&E staining, (C) SEM and (D) AFM images of tendon cryosection. (E) Morphology of cells on tendon cryosection, and on glass were revealed by live/dead staining. Green fluorescence indicates living cells seeded on the sections, and red fluorescence reveals dead endogenous cells in the tendon. (F) Quantification of the elongation of cells cultured on tendon histological sections (shaded bars) and on glass surface (solid bars). MC3T3E1 (blue), 3T3 (green), htMSC (grey), MDCK (orange) and HeLa (red) were used. Elongation of cells was measured as aspect ratios, defined as the major axis/minor axis of individual cell. At lease 100 cells were randomly measured for each cell line (*represents $p < .05$). (For interpretation of the references to colour in this figure legend, the reader is referred to the web version of this article.)

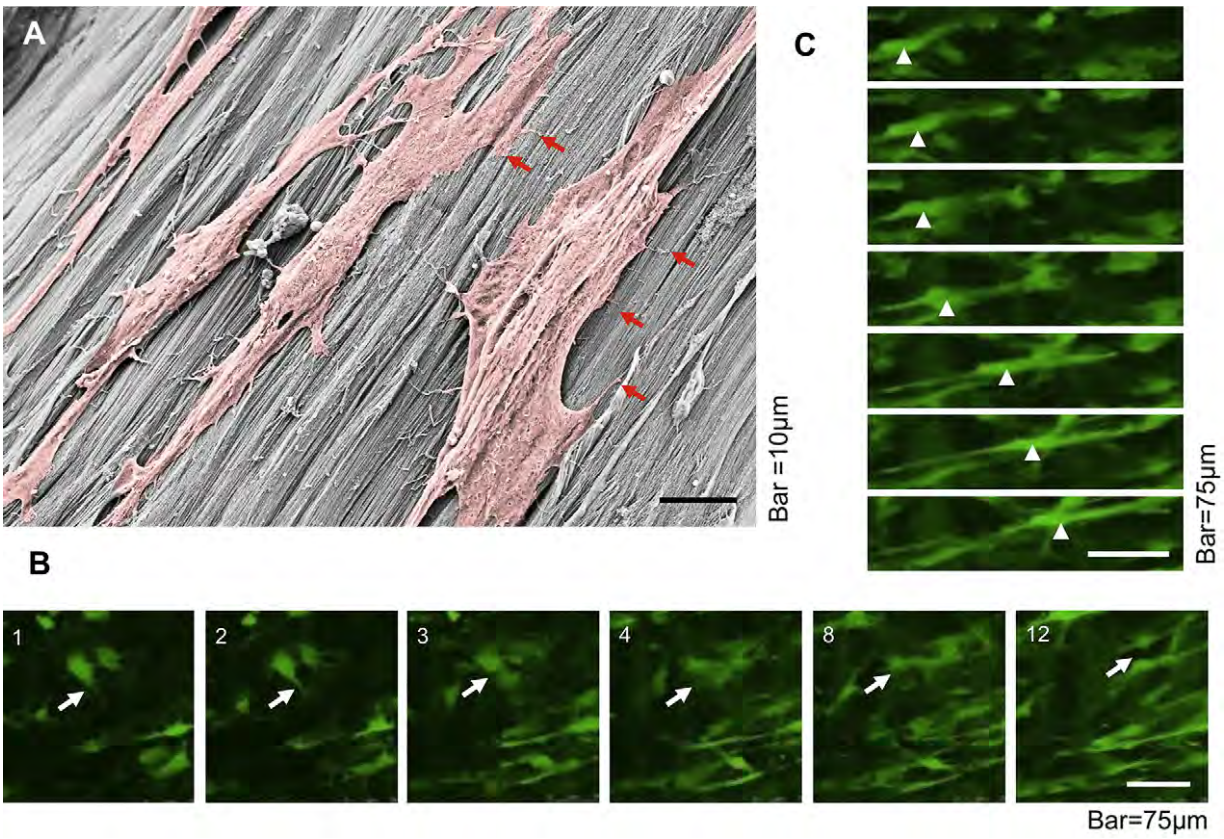

Fig. 2. (A) SEM image of MSCs attached on tendon cryosection. MSC highlighted in pink pseudocolor. (B&C) Time-lapse microscopy of MSCs seeded on the tendon sections. (B) Snapshots of the dynamics of filopodia projections over 12 h period. The numbers signify the number of hours after seeding. (B) Snapshots of the elongation dynamics of one MSC (arrowhead) on section within 6 h. Please refer to the supplement for the full time-lapse movie. (For interpretation of the references to colour in this figure legend, the reader is referred to the web version of this article.)

3 h of MSC spreading, the filopodia projected and retracted in all directions on the sections (Fig. 2B). Afterwards, filopodia around cells perpendicular to the fibrils dynamically retracted (Fig. 2B, arrows) and the cell elongation axis was established at this point. Most of the cells on the section were elongated after about 4 h. Interestingly, cells were surprisingly dynamic, moving along collagen fibrils over as much as 100 μm within 6 h (Fig. 2C, arrowheads). This agility is consistent with our SEM observation that cells were not deeply entrenched in the section, but attached to the collagen fibres at a small number of sites (Fig. 2A). The high mobility of MSCs on the section may represent the transient nature of the interactions between the cells and the collagen fibres. The dynamic nature of cell elongation shown in timelapse imaging also explains the apparently high variability of cellular aspect ratio measurement (e.g., Fig. 1F).

3.3. Tendon cryosections promote cell lineage commitment

The striking elongation of MSC cultured on tendon sections prompted us to investigate the proliferation and differentiation properties of these cells. The proportion of cells in the S-phase of the cell cycle was quantified by using EdU pulse labelling. MSC cultured on tendon sections exhibit a lower rate of DNA synthesis as compared to the cells on glass (Fig. 3A). The decrease in cell proliferation on tendon sections implies that these cells might commit to differentiation more efficiently. We examined the expression of TNMD, a commonly used tenocyte marker [25], in MSC on tendon sections and on glass (Fig. 3B). We chose an antibody that does not react with bovine TNMD (Fig. 3C), hence ensuring that the endogenous TNMD in the sections did not interfere with the detection of human TNMD expression in the MSC. Remarkably, MSC on section expressed around 1.5 fold higher level of TNMD compared on glass as early as 3 days, and the difference increased to 2.5 fold at day 12 of culture (Fig. 3B). TNMD expression in most of the cells cultured on glass was significantly weaker than that of on the section throughout the experiment (Fig. 3D–E). Therefore, the surface of tendon sections contains sufficient information that can guide MSC to the tenocyte lineage, without the need for any exogenous growth factors.

3.4. Exposed physical architecture and biochemical details dictate cell fate

Our data indicate that histological sections of tendon provide a unique surface that guides the alignment, elongation and differentiation of MSC. This experimental model provides a unique system for the evaluation of the functional importance of various aspects of TME.

First, we investigated the role of the physical architecture on the surface of tendon sections in MSC behaviours. It is difficult to detangle the complex biochemical and physical information in a TME, but tendon provides a simple solution to this challenge. As tendon is a highly structured tissue, sections with distinct surface architectures can be generated by simply varying the cutting angle (Fig. 4A). For example, when the tendon is transversely sectioned, the resulting sections appear strikingly different from the longitudinal sections. Instead of exhibiting the characteristic collagen fibrils, the cross sections have a relatively smooth morphology

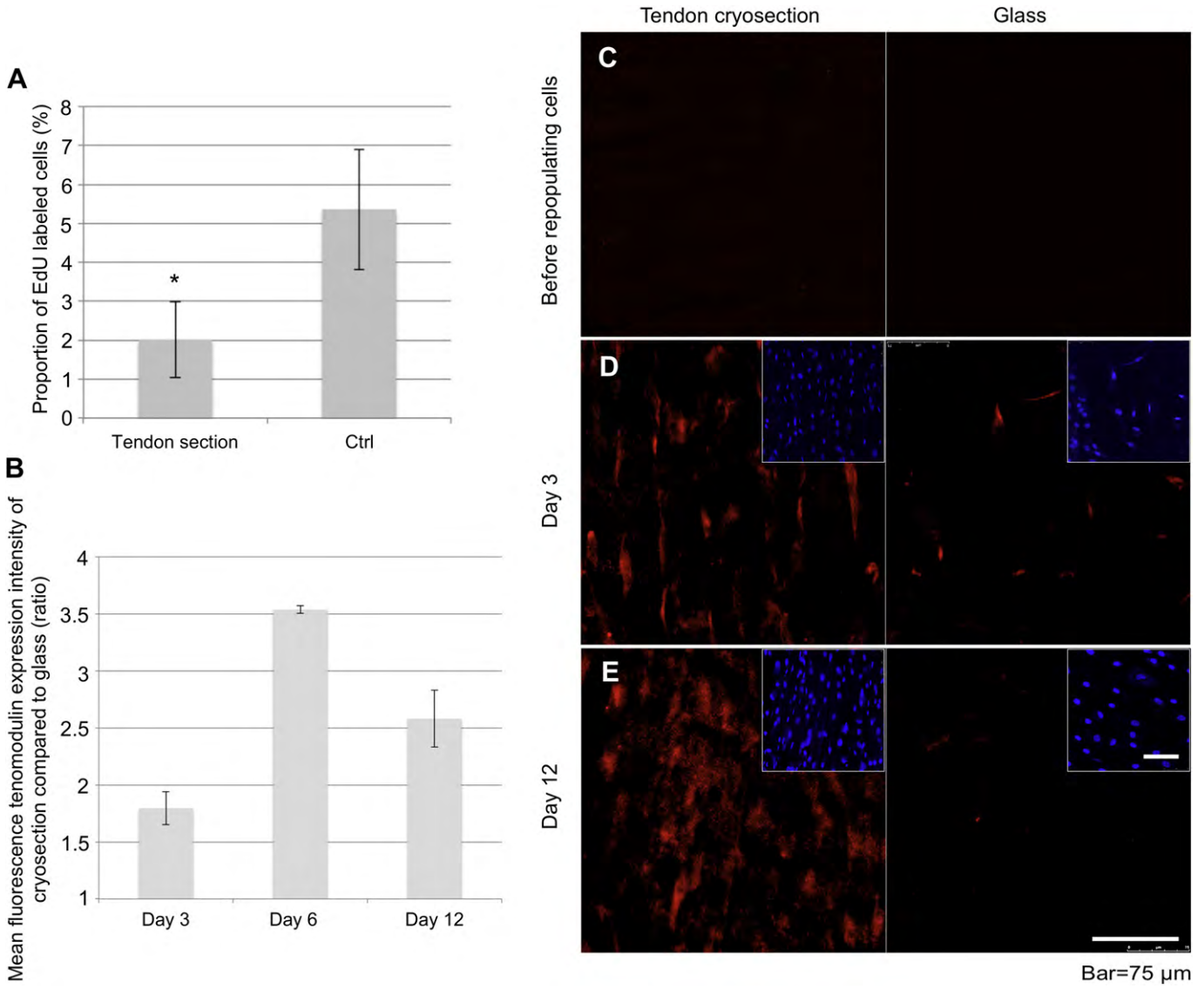

Fig. 3. (A) EdU proliferation assay of MSCs on tendon section and glass. (B) Tenomodulin expression intensity measurements over 12 days of culture. (C) Immunofluorescence of tenomodulin in MSCs on day 3, 6 and 12 post-seeding, the inset shows Hoechst staining of cells. (blue: nuclei; red: tenomodulin) (*represents $p < .05$ compared to other groups). (For interpretation of the references to colour in this figure legend, the reader is referred to the web version of this article.)

(Fig. 4B). Despite their difference in surface topography, "cross-cut" (CC) and "longitudinally cut" (LC) sections contain similar number of cells (Fig. 4C) and virtually indistinguishable protein composition, as judged by gel electrophoresis (Fig. 4D). The abundances of fibronectin and collagen I, two archetypal ECM proteins, in these two types of sections are also highly similar (Fig. 4D). This allows us to define the role of physical architecture of TME.

When MSC were seeded on CC sections, they demonstrated no significant alignment, elongation and TNMD expression when compared to cells cultured on LC sections (Fig. 4E–G). Western blotting analysis also showed a higher expression of TNMD, but not SOX9 and ALP, in MSC on LC section than cells on either CC sections or on glass (Fig. 4G). This indicates that while LC section contains the instructive niche that supports MSC differentiation into the tenocytic, but not osteogenic or chondrogenic lineages, this niche is lost on the CC section. Hence, the removal of the physical architecture effectively abolishes the functions of a TME. As LC and CC contain a similar abundance of fibronectin and collagen I (Fig. 4D), our observation further suggests that the physical presentation of the ECM is more important than the net concentration of ECM components in determining cell differentiation. Stress fibres, as indicated by Phalloidin staining, appeared more pronounced in MSC on the LC than on the CC section or glass surface (Fig. 4H). In addition, the expression of integrin β1, and not integrin α3 (Suppl Fig. 3), on MSC was significantly stronger on the LC than on the CC section. This suggests a role of integrin β1 in the signalling between cells and the tendon TME. Thus, differences in the surface topography of tendon sections induce different responses in cell morphology, adhesion and cytoskeleton.

We performed a series of experiments to interrogate various aspects of the TME presented on the LC section and other roles in controlling MSC morphology and differentiation (Fig. 5). First, we investigated the possible roles of biochemical signals present in the TME. Cell adhesion assay showed that cells attach more efficiently on the LC than on the CC section (Suppl Fig. 4). This difference in cell adhesion efficiency was dramatically reduced (Suppl Fig. 4) when the sections were pre-incubated with 10% BSA (Fig. 5, step 1), which suggests that the cell-binding sites on the LC section could be masked by non-specific protein blocking. Hence, both the physical architecture and biochemical cues exposed on LC tendon section

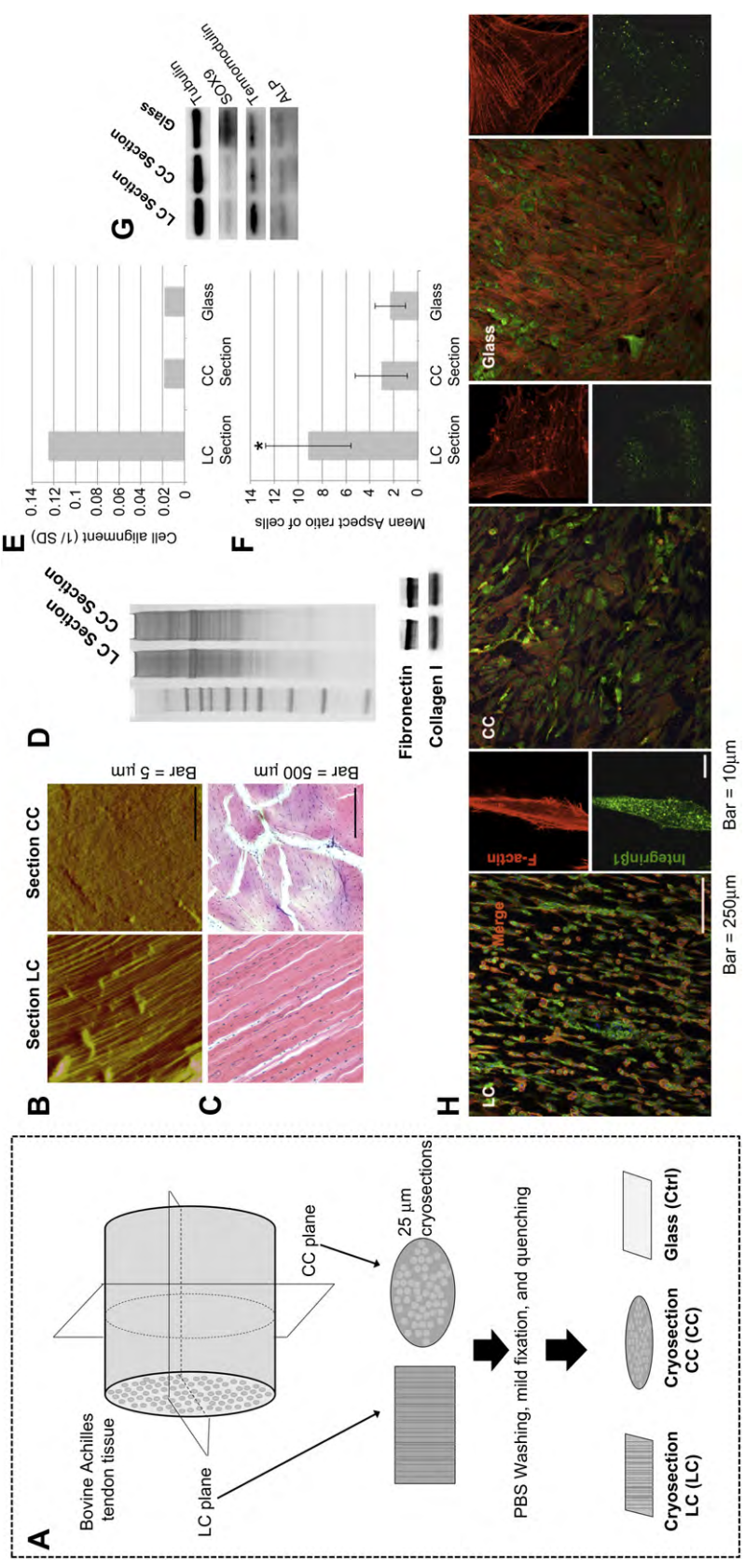

Fig. 4. (A) Schematic diagram of cryosection preparation at longitudinal (LC) and crosssectional (CC) plane. (B) AFM and (C) H&E images of cryosections prepared in this manner. (D) Coomassie blue staining of proteins extracted from the sections and separated by SDS-PAGE. Expression of fibronectin and collagen I in these sections is analysed by western blotting. Morphology of MSC adhered on the cryosections illustrated by (E) cell alignment and (F) cell elongation. (G) Western blotting of MSCs on day 3 against sox9, tenomodulin and alkaline phosphatase. (H) Immunofluorescence of integrin β1 (green) of MSCs 3 days after seeding on the cryosections and glass. Phalloidin actin fibre staining and Hoechst DNA staining are labelled by red and blue, respectively. The inset shows the immunofluorescence at high magnification. (For interpretation of the references to colour in this figure legend, the reader is referred to the web version of this article.)

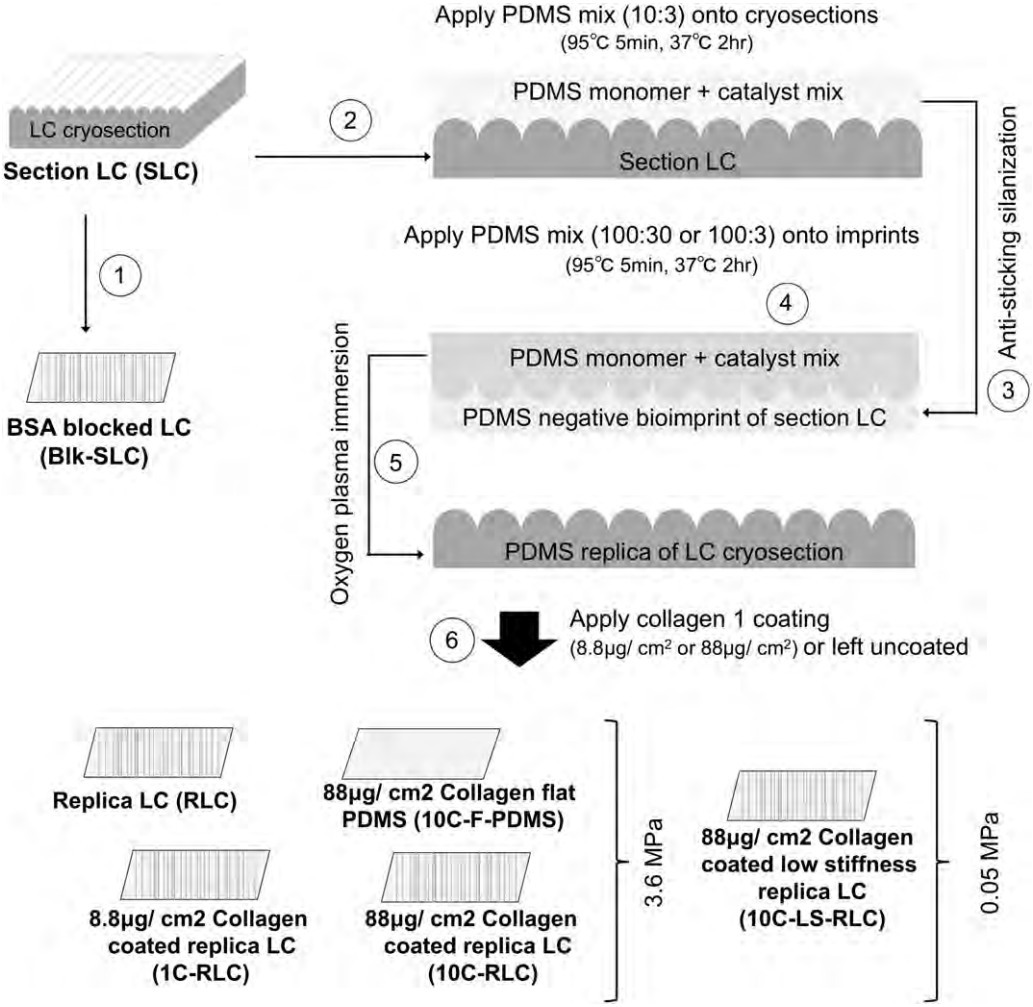

Fig. 5. Schematic diagram of the LC cryosection replica fabrication using bioimprinting and coating techniques.

dictates adhesion, morphology, proliferation and lineage commitment of stem cells.

3.5. PDMS bioimprints reconstructed the essential details of TME and restored its function

To faithfully reconstruct the physical components of the LC TME, we used tendon LC cryosections as the template on which PDMS was polymerised (Fig. 5, Step 2). This method has been used to prepare imprints of cell surfaces for AFM studies [19]. Here, we utilised this approach to make bioimprints of LC tendon sections. The resulting bioimprints could then be used as a negative replica for a second round of PDMS imprinting (Fig. 5, Step 4) with the aid of anti-sticking silanization (Fig. 5, Step 3), which produced a positive copy of the original template. As the hydrophobicity of PDMS is incompatible with cell culture, we modified the surface of the imprinted tendon replica by a plasma immersion process (Fig. 5, Step 5) that effectively increased its wettability (Fig. 6A). The overall topography of the replica under an optical microscope was very similar to that of the LC tendon cryosection (Fig. 6C). AFM measurements also showed that the groove pitch and width of the bioimprint were similar to the submicron details of the original section template (Fig. 6D). These bioimprints therefore represent a faithful reproduction of the surface topography of the LC sections. Furthermore, by adjusting the ratio of the base and curing agent, we were able to synthesise tendon section replicas with different mechanical properties. Fig. 6B shows the AFM indention measurements of three PDMS replica prepared from different monomer–catalyst combinations. The surface topography of these replicas was virtually identical (Fig. 6C). The Young's modulus of the replica produced by using "100:30" mix was 3.5 MPa, close to the literature value of the hydrated tendon measured by AFM indentation [26,27].

MSC seeded on BSA-blocked LC (Blk-SLC) sections and on PDMS LC replica (RLC) adopted an elongated and aligned morphology as on the tendon section LC (SLC) (Fig. 7A–C). However, MSC did not express TNMD (Fig. 6D) on either surface, even after 6 days of culture. Hence, cell morphology and differentiation appear to be influenced by different sets of factors: the physical topography of TME is sufficient to induce changes in cell shapes, but specific saturable biochemical cues is necessary for differentiation. To further demonstrate this point, we cultured MSC on a nanogrooved titanium surface (Suppl Fig. 5), an inert substrate that is known to induce cell alignment and elongation [28]. The surface topography of the titanium was adjusted so that the resulting shape and alignment of MSC cultured was similar to those seeded on tendon LC section (Suppl Fig. 5A). However, the TNMD expression of these cells was not significantly increased (Suppl Fig. 5B). Hence, the manipulation of MSC into a specific cell shape does not necessarily accompany differentiation. It is clear that although the bioimprint of tendon LC cryosection successfully replicated its sub-micron

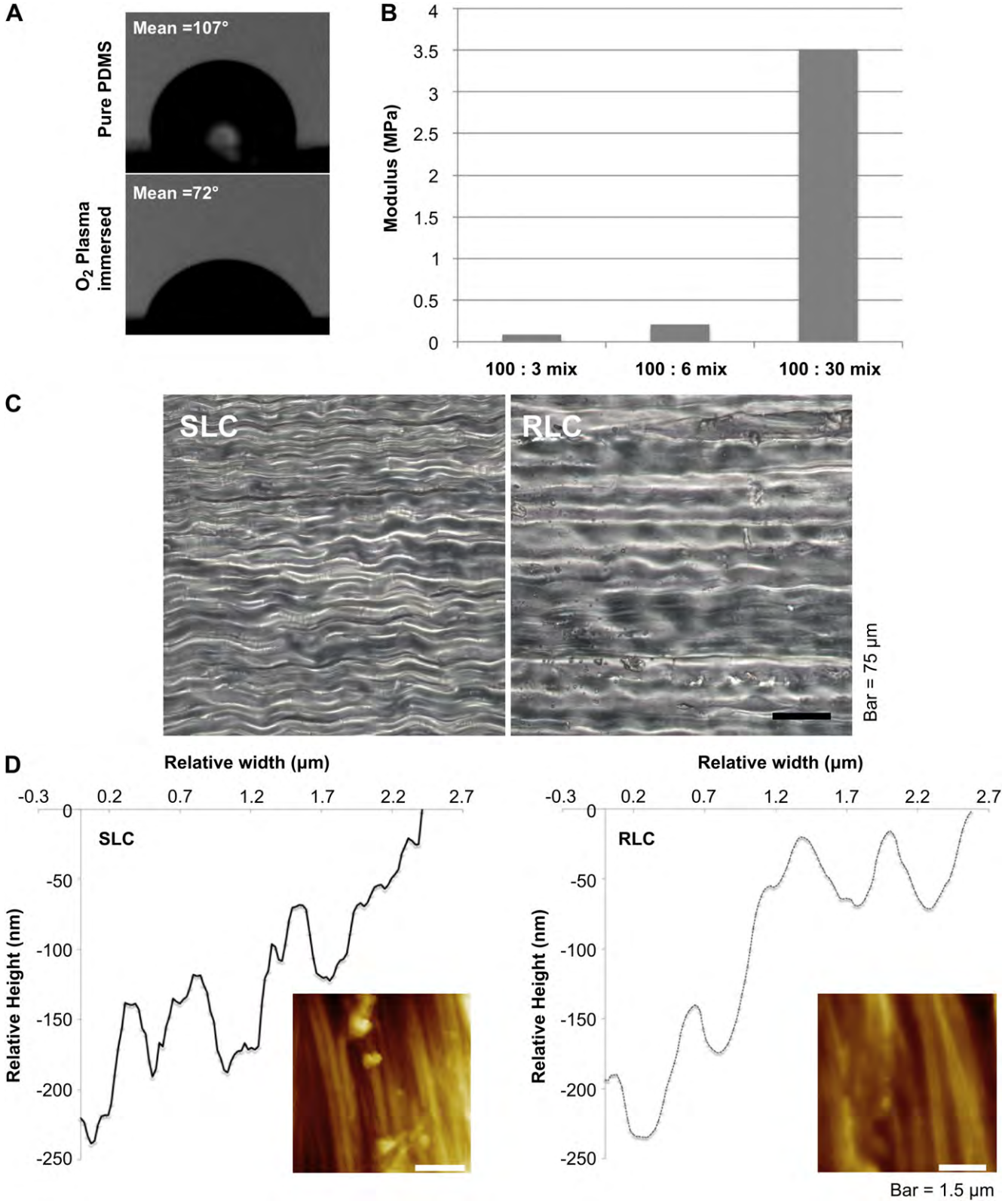

Fig. 6. (A) Water contact angle measurement of the pure and O_2 plasma immersed PDMS. (B) Young's modulus measurement on PDMS at various curing agent concentration. (C) Low magnification bright field images of the cryosection LC (SLC) and the replica LC (RLC). (D) Surface topography of SLC and RLC as measured by AFM. Inset: High magnification images.

scale topography to control MSC morphology, the missing of biochemical cues renders the information incomplete.

Since the PDMS replica of the LC tendon section provides a faithful reproduction of the physical features of LC TME, biochemical coatings could be easily applied to provide both physical and biochemical cues simultaneously. As the major ECM component in tendon is collagen 1 [29,30], we applied tendon collagen 1 as the biochemical coating of the replica (Fig. 5, Step 6).

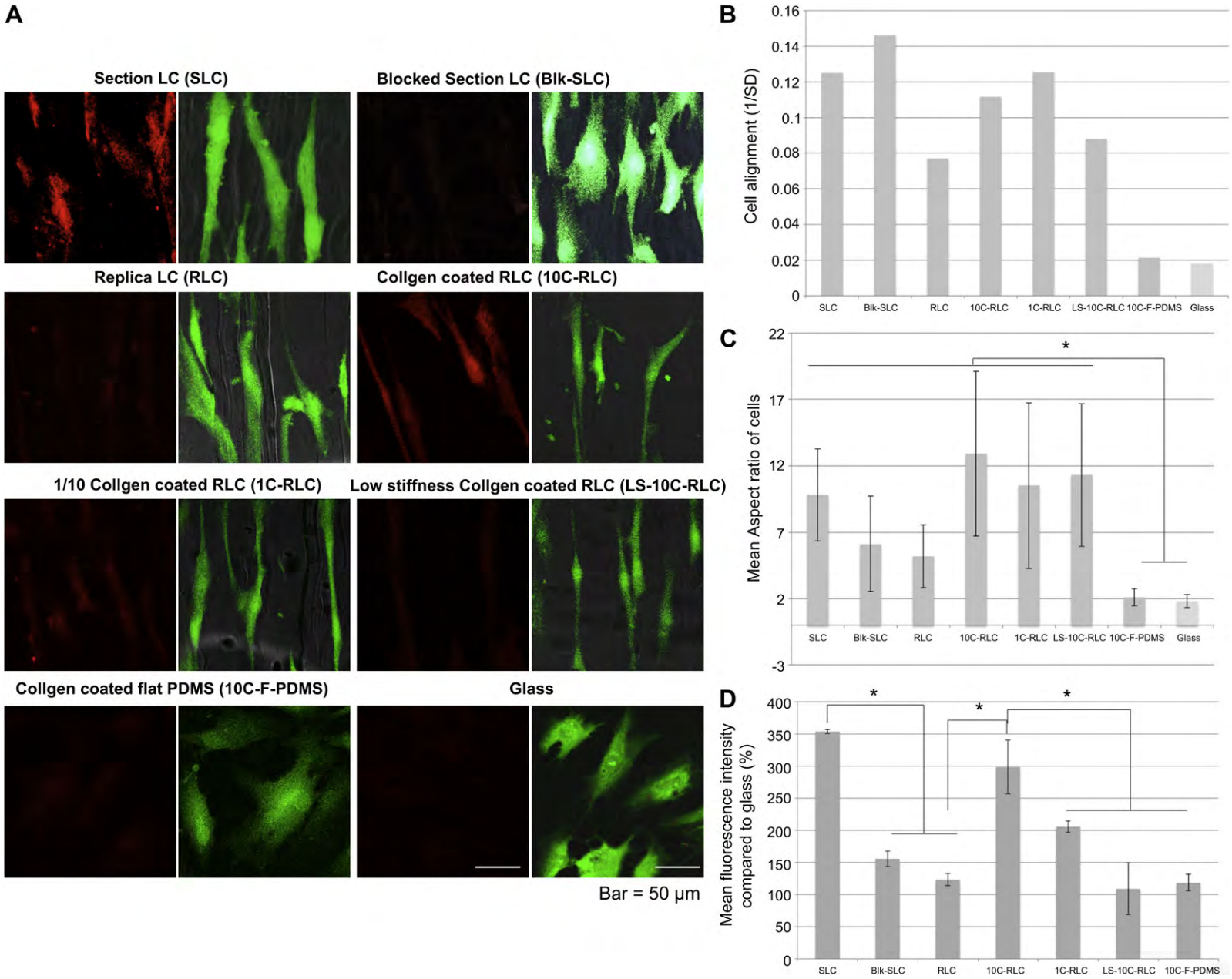

Fig. 7. (A) Confocal microscopy of the immunofluorescence against tenomodulin and GFP of MSC cultured on cryosection LC (SLC), BSA-blocked SLC, Replica LC (RLC), collagen coated RLC (10C-RLC), low concentration collagen coated RLC (1C-RLC), low modulus and collagen coated RLC (LS-10C-RLC), collagen coated flat PDMS (10C-F-PDMS) and glass surface. (B) Measurement of MSC alignment on the substrates. (C) Measurement of MSC elongation on the substrates. (D) Tenomodulin expression intensity measurements of MSC on the substrates. (*represents $p < .05$ compared to the indicated groups).

As shown in Fig. 7D, collagen 1 coating on the bioimprint (10C-RLC), can effectively induce TNMD expression in MSC. It appears that the effect of collagen 1 is concentration dependent, as a reduction of the amount of collagen 1 (1C-RLC) results in the loss of TNMD induction. In consistent with our observation on the importance of the surface topography, coating of flat PDMS with collagen 1 (10C-F-PDMS) did not lead to MSC differentiation.

Next we examined the effect of the physical elasticity of the tendon bioimprint on MSC morphology and differentiation. By varying monomer concentrations, we can produce PDMS bioimprints with different elasticity, while retaining the same surface architecture and collagen coating. Here we tested a bioimprints with similar stiffness (3.5 MPa) to bovine tendon [27], and one with much less stiffness (0.35 MPa). The softer bioimprint, LS-10C-RLC, can still support MSC alignment and elongation, but failed to promote an upregulation of TNMD (Fig. 6D).

Taken together, we have tested the importance of various aspects of TME to MSC morphology and differentiation. We discovered that for MSC to commit to the tenocyte lineage, the simultaneous presence of three factors is necessary: the right physical architecture, the right ECM and the right stiffness. The tendon cryosection exposed at LC contain the correct presentation of theses three factors. By the fabrication of materials that replicates all three factors with bioimprinting and coating techniques, we have successfully reconstructed the tendon LC TME that has the instructive effect on the tenogenic differentiation of MSC.

4. Discussion

Inside a tissue, each cell is intimately enveloped in a microenvironment that harbours both the biophysical and biochemical signalling cues necessary for maintaining and regulating the cell's physiological functions. Here, we have developed a simple and innovative system to define how natural TME modulates cell phenotypes. The two major discoveries reported in this study are: (1) histological sections of a tissue, represented here by bovine Achilles tendon, contain sufficient signals that can instruct the differentiation of MSC into the corresponding cell type in that tissue, and (2) it is possible to reconstruct these signals by bioimprinting and ECM coating. Although we focused our study on Achilles tendon, it is possible that this approach can be extended to other organs, as we observed that MSC adopted highly different morphology on sections cut from different tissues. The implication of these findings is that it may be possible to artificially reproduce a diverse variety of tissue niches by bioimprinting tissue sections and by coating these imprinted surfaces with the right ECM components.

The data shown in this study demonstrate that stem cell lineage commitment can be driven by tissue sections. Other protocols for the induction of MSCs undergo tenogenesis involve the use of a co-culture system with primary tendon fibroblasts [31], mechanical stimulation [32,33] or nano-fibres supplemented with growth factors [34]. More recently, Kishore et al. [35] have reported that the tenogenic differentiation of MSCs can be induced by a biomaterial containing electrochemically aligned collagen threads without the addition of growth factors, suggesting that aligned collagen fibrils can mimic the native tendon TME. However, the fabrication of surfaces that harbour highly aligned collagen proteins is relatively tedious and technically challenging. Our study suggests that histological sections of tendon already contain all these biochemical and extracellular information to induce the morphological and functional reprogramming of MSC. To date, the most physiological representation of TME comes in the form of decellularised organs. However, the harsh decellularisation procedures inevitably lead to the disruption of the tissue architecture (Suppl Fig. 1), preventing a detailed analysis of TME functions and properties. In our system, the TME is much more faithfully preserved. The tendon sections were shown to contain closely packed fibres that are similar to the native tendon tissues in terms of dimension and density [36,37]. The elasticity measured by AFM mapping is also comparable with the published data on hydrated collagen fibrils [26,27]. Although natural TME is a 3D microenvironment [38], we intentionally devised a more convenient 2D culture system, that enables the visualisation of cell-TME interactions (Fig. 2A), and characterization by time-lapse microscopy the dynamics of cells on the TME (Fig. 2B and C).

To faithfully replicate biophysical details of the TME, we used nanoimprinting to replicate patterns at high resolution and at low cost. Similar imprinting by polymerisation on fixed cultured cells has been used to copy the ultrastructural contour of cell surfaces for imaging [39]. Muys et al. reported that PDMS imprinting preserved the cellular physical details as small as 100 nm as revealed by AFM [19]. Here, we extended the use of this technique to replicate the detailed topography of TME, by optimizing the technique to produce a positive replica of a tissue (Fig. 5). We successfully demonstrated that it is possible to fabricate a replica that precisely reproduced the physical dimension and topography of a tendon section at sub-micron levels (Fig. 6C and D). MSC were shown to adopt as elongated and aligned as they do on LC tendon cryosections, implicating that the replica possessed the function contact guidance as seen on LC sections. Importantly, collagen I extracted from rat tail tendon, when coated on the replica, can induce the differentiation of MSC into tenocytes.

Our data open many new avenues for future investigations. For example, it will be interesting to study whether different types of collagen have the same effect on promoting tenocytic differentiation. We can answer this question by coating the bioimprinted tendon replica with the collagen extracted from different organs. In fact, the TME replica, essentially a biomimetic cell culture substrate, provides a platform for screening the biological properties of ECM components. Many "ECM array" experiments have been done to screen for ECM components important for directing stem cell differentiation. However, in these studies, the ECM proteins are presented to the cells on flat protein surfaces [14] or in hydrogels [40]. Thus, the physical and textural information of TME is lost. Our replicas should enable these screening exercises to be done in a correct structural context.

Another question arisen from our study is the importance of the orientation of collagen fibres in influencing cell differentiation. Most collagen coating procedure do not control or specify the orientation of these protein molecules on cell culture surfaces. Our experiments on the LC and CC tendon sections suggested that it is the precise orientation of collagen fibrils, not the amount of collagen protein, that effects MSC alignment, elongation and differentiation. Similarly, collagen I coated PDMS slab did not support tenocytic differentiation, which occurred only when the same amount of collagen I was coated on the PDMS replica of tendon section. Future study will clarify whether the replica could control the orientation of collagen fibrillogensis.

Our observations on the properties of tissue sections and their replicas suggest that three interrelated factors contribute to the functions of TME: precise topographical pattern, correct ECM component and mechanical characteristics (Fig. 8). The absence, or incorrect dose, of either factor will abolish the TME. Such a delicate balance coincides with some earlier observations in tenogenesis. MSC are influenced to commit to the tenogenic lineage when cultured on collagen-coated substrate with a suitable elasticity [32] or on a fibrous scaffold [41]. Consistent with this concept, Yamming et al. recently showed that the deletion of ECM proteins Bgn and Fmod, results in the malformation of the tendon architecture,

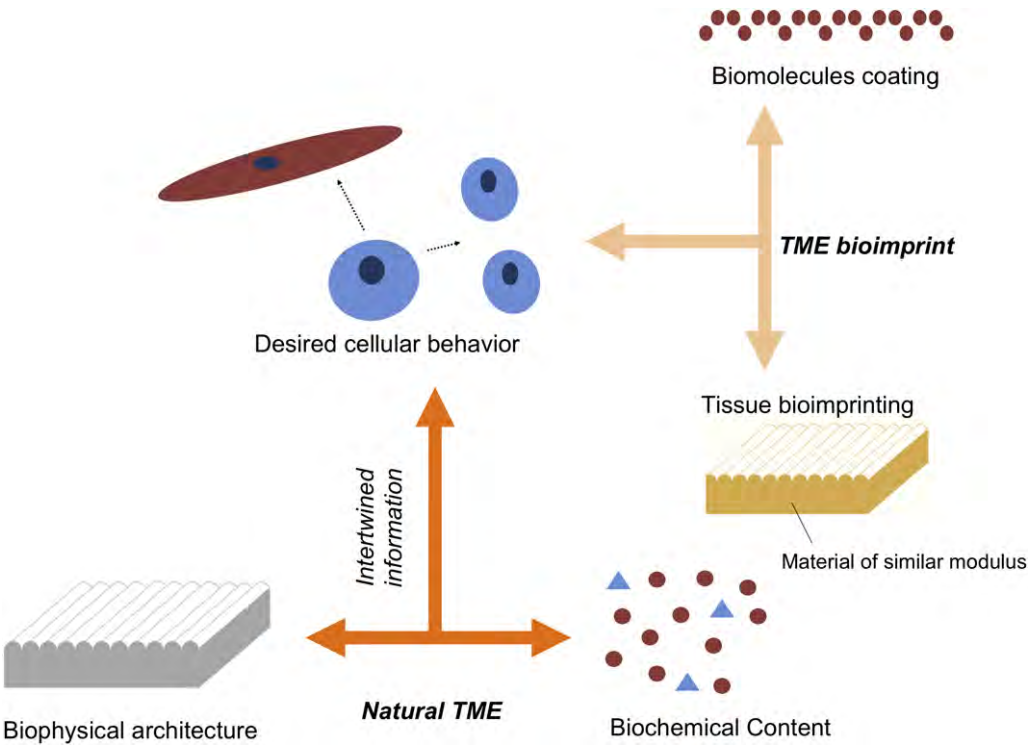

Fig. 8. Summary of this study.

which in turn leads to the possible destruction of the tendon stem cell niche [42]. This study shows that the combination of bioimprinting and ECM coating provides a convenient way to replicate the functionality of the TME. Our preliminary data indicate that MSC adopt distinct morphology when seeded on bone and cartilage sections (Fig. 1A), implying that this experimental regime can potentially be extended to other organs. To functionally copy a TME, two pieces of information will be required: the stiffness of the tissue at its native state and the biochemical composition of its ECM. As these data can readily be obtained by using such techniques as AFM and proteomics, we envisage that the approach reported in this study can be systematically applied to other, more complex, tissues.

5. Conclusion

Current biomaterials lack the complexity and functionality of the natural TME, nor do they reflect the dimensions of tissue TME found in nature. The experimental models described in this study provide a simple and convenient paradigm to functionally define a TME. By combining the correct ECM component and a bioimprint with the correct mechanical properties (Fig. 8), we have demonstrated the feasibility of replicating a TME with artificial materials that possess the capability to guide specific cell behaviour. We envisage that this model can be conveniently extended to study and reconstruct the microenvironment in other normal, diseased or regenerating tissues. We believe this study provides a simple yet useful solution to meet the current challenge of the tissue engineering field.

Acknowledgements

This study is supported by CityU Strategic Research Grants (numbers 7008084 and 7002573) and Hong Kong Research Grant Council General Research Fund (number 123708 and 9041410). We thank Mr Michael Chiang (Department of Biology and Chemistry, City University of Hong Kong) for his help in the SEM experiments, Dr Alice Wong (School of Biological Sciences, The University of Hong Kong) for her useful comments and anti-Integrin antibodies, Prof. Joseph Wong (Division of Life Science, Hong Kong University of Science and Technology) for the use of AFM, and all members of the Lam and the Yeung Labs for their ideas, discussion and encouragement.

Appendix A. Supplementary data

Supplementary data related to this article can be found online at http://dx.doi.org/10.1016/j.biomaterials.2012.07.002.

References

[1] Bruder SP, Fox BS. Tissue engineering of bone. Cell based strategies. Clin Orthop Relat Res 1999;(367 Suppl):S68–83.
[2] Kim D-H, Provenzano PP, Smith CL, Levchenko A. Matrix nanotopography as a regulator of cell function. J Cell Biol 2012;197(3):351–60.
[3] Dvir T, Timko BP, Kohane DS, Langer R. Nanotechnological strategies for engineering complex tissues. Nat Nanotechnol 2011;6(1):13–22.
[4] Kshitiz Kim DH, Beebe DJ, Levchenko A. Micro- and nanoengineering for stem cell biology: the promise with a caution. Trends Biotechnol 2011;29(8):399–408.
[5] Evans ND, Gentleman E, Chen X, Roberts CJ, Polak JM, Stevens MM. Extracellular matrix-mediated osteogenic differentiation of murine embryonic stem cells. Biomaterials 2010;31(12):3244–52.
[6] Biggs MJP, Richards RG, Dalby MJ. Nanotopographical modification: a regulator of cellular function through focal adhesions. Nanomedicine 2010;6(5):619–33.
[7] Yim EK, Reano RM, Pang SW, Yee AF, Chen CS, Leong KW. Nanopattern-induced changes in morphology and motility of smooth muscle cells. Biomaterials 2005;26(26):5405–13.
[8] Curran JM, Chen R, Stokes R, Irvine E, Graham D, Gubbins E, et al. Nanoscale definition of substrate materials to direct human adult stem cells towards tissue specific populations. J Mater Sci Mater Med 2010;21(3):1021–9.
[9] Flynn LE. The use of decellularized adipose tissue to provide an inductive microenvironment for the adipogenic differentiation of human adipose-derived stem cells. Biomaterials 2010;31(17):4715–24.

[10] Holst J, Watson S, Lord MS, Eamegdool SS, Bax DV, Nivison-Smith LB, et al. Substrate elasticity provides mechanical signals for the expansion of hemopoietic stem and progenitor cells. Nat Biotechnol 2010;28(10):1123–8.
[11] Martin JY, Schwartz Z, Hummert TW, Schraub DM, Simpson J, Lankford Jr J, et al. Effect of titanium surface roughness on proliferation, differentiation, and protein synthesis of human osteoblast-like cells (MG63). J Biomed Mater Res 1995;29(3):389–401.
[12] Schneider GB, Perinpanayagam H, Clegg M, Zaharias R, Seabold D, Keller J, et al. Implant surface roughness affects osteoblast gene expression. J Dent Res 2003;82(5):372–6.
[13] Mei Y, Saha K, Bogatyrev SR, Yang J, Hook AL, Kalcioglu ZI, et al. Combinatorial development of biomaterials for clonal growth of human pluripotent stem cells. Nat Mater 2010;9(9):768–78.
[14] Flaim CJ, Chien S, Bhatia SN. An extracellular matrix microarray for probing cellular differentiation. Nat Methods 2005;2(2):119–25.
[15] Fleming JM, Miller TC, Quinones M, Xiao Z, Xu X, Meyer MJ, et al. The normal breast microenvironment of premenopausal women differentially influences the behavior of breast cancer cells in vitro and in vivo. BMC Med 2010;8:27.
[16] Engler AJ, Richert L, Wong JY, Picart C, Discher DE. Surface probe measurements of the elasticity of sectioned tissue, thin gels and polyelectrolyte multilayer films: correlations between substrate stiffness and cell adhesion. Surf Sci 2004;570(1–2):142–54.
[17] Engler AJ, Carag-Krieger C, Johnson CP, Raab M, Tang HY, Speicher DW, et al. Embryonic cardiomyocytes beat best on a matrix with heart-like elasticity: scar-like rigidity inhibits beating. J Cell Sci 2008;121(Pt 22):3794–802.
[18] Mihara K, Imai C, Coustan-Smith E, Dome JS, Dominici M, Vanin E, et al. Development and functional characterization of human bone marrow mesenchymal cells immortalized by enforced expression of telomerase. Br J Haematol 2003;120(5):846–9.
[19] Muys JJ, Alkaisi MM, Melville DOS, Nagase J, Sykes P, Parguez GM, et al. Cellular transfer and AFM imaging of cancer cells using bioimprint. J Nanobiotechnology 2006;4(1):1.
[20] Wang H, Ji J, Zhang W, Wang W, Zhang Y, Wu Z, et al. Rat calvaria osteoblast behavior and antibacterial properties of O_2 and N_2 plasma-implanted biodegradable poly(butylene succinate). Acta Biomater 2010;6(1):154–9.
[21] Kim B, KP ET, Papautsky I. Long-term stability of plasma oxidized PDMS surfaces. Conf Proc IEEE Eng Med Biol Soc 2004;7:5013–6.
[22] Omae H, Zhao C, Sun YL, An KN, Amadio PC. Multilayer tendon slices seeded with bone marrow stromal cells: a novel composite for tendon engineering. J Orthop Res 2009;27(7):937–42.
[23] Ott HC, Matthiesen TS, Goh S-K, Black LD, Kren SM, Netoff TI, et al. Perfusion-decellularized matrix: using nature's platform to engineer a bioartificial heart. Nat Med 2008;14(2):213–21.
[24] Gilbert TW, Sellaro TL, Badylak SF. Decellularization of tissues and organs. Biomaterials 2006;27(19):3675–83.
[25] Docheva D, Hunziker EB, Fässler RR, Brandau O. Tenomodulin is necessary for tenocyte proliferation and tendon maturation. Mol Cell Biol 2005;25(2):699–705.
[26] Grant CA, Brockwell DJ, Radford SE, Thomson NH. Tuning the elastic modulus of hydrated collagen fibrils. Biophys J 2009;97(11):2985–92.
[27] Grant CA, Brockwell DJ, Radford SE, Thomson NH. Effects of hydration on the mechanical response of individual collagen fibrils. Appl Phys Lett 2008; 92(23):233902–3.
[28] Yang SP, Lee TM. The effect of substrate topography on hFOB cell behavior and initial cell adhesion evaluated by a cytodetacher. J Mater Sci Mater Med 2011; 22(4):1027–36.
[29] Bank RA, TeKoppele JM, Oostingh G, Hazleman BL, Riley GP. Lysylhydroxylation and non-reducible crosslinking of human supraspinatus tendon collagen: changes with age and in chronic rotator cuff tendinitis. Ann Rheum Dis 1999;58(1):35–41.
[30] Riley GP, Harrall RL, Constant CR, Chard MD, Cawston TE, Hazleman BL. Tendon degeneration and chronic shoulder pain: changes in the collagen composition of the human rotator cuff tendons in rotator cuff tendinitis. Ann Rheum Dis 1994;53(6):359–66.
[31] Schneider PRA, Buhrmann C, Mobasheri A, Matis U, Shakibaei M. Three-dimensional high-density co-culture with primary tenocytes induces tenogenic differentiation in mesenchymal stem cells. J Orthop Res 2011;29(9): 1351–60.
[32] Sharma RI, Snedeker JG. Biochemical and biomechanical gradients for directed bone marrow stromal cell differentiation toward tendon and bone. Biomaterials 2010;31(30):7695–704.
[33] Farng E, Urdaneta AR, Barba D, Esmende S, McAllister DR. The effects of GDF-5 and uniaxial strain on mesenchymal stem cells in 3-D culture. Clin Orthop Relat Res 2008;466(8):1930–7.
[34] Sahoo S, Toh SL, Goh JCH. A bFGF-releasing silk/PLGA-based biohybrid scaffold for ligament/tendon tissue engineering using mesenchymal progenitor cells. Biomaterials 2010;31(11):2990–8.
[35] Kishore V, Bullock W, Sun X, Van Dyke WS, Akkus O. Tenogenic differentiation of human MSCs induced by the topography of electrochemically aligned collagen threads. Biomaterials 2012;33(7):2137–44.
[36] Lee GJ, Choi S, Chon J, Yoo S, Cho I, Park HK. Changes in collagen fibril pattern and adhesion force with collagenase-induced injury in rat Achilles tendon observed via AFM. J Nanosci Nanotechnol 2011;11(1):773–7.
[37] Orgel JPRO, San Antonio JD, Antipova O. Molecular and structural mapping of collagen fibril interactions. Connect Tissue Res 2010;52(1):2–17.
[38] Deforest CA, Anseth KS. Advances in bioactive hydrogels to probe and direct cell fate. Annu Rev Chem Biomol Eng 2012;3:421–44.
[39] Nock V, Murray L, Samsuri F, Alkaisi MM, Evans JJ. Microfluidics-assisted photo nanoimprint lithography for the formation of cellular bioimprints. J Vac Sci Technol B 2010;28(6). C6K17–C6K22.
[40] Benoit DS, Schwartz MP, Durney AR, Anseth KS. Small functional groups for controlled differentiation of hydrogel-encapsulated human mesenchymal stem cells. Nat Mater 2008;7(10):816–23.
[41] Yin Z, Chen X, Chen J, Shen W, Hieu NT, Gao L, et al. The regulation of tendon stem cell differentiation by the alignment of nanofibers. Biomaterials 2010; 31(8):2163–75.
[42] Bi Y, Ehirchiou D, Kilts T, Inkson C, Embree M, Sonoyama W, et al. Identification of tendon stem/progenitor cells and the role of the extracellular matrix in their niche. Nat Med 2007;13(10):1219–27.